

Dependences of the X-ray luminosity and pulsar wind nebula on different parameters of pulsars and the evolutionary effects

Oktay H. Guseinov^{1,2} *, Aşkın Ankay¹ †,
Sevinç O. Tagieva³ ‡; M. Özgür Taşkın⁴ §

¹TÜBİTAK Feza Gürsey Institute
81220 Çengelköy, İstanbul, Turkey

²Akdeniz University, Physics Department,
Antalya, Turkey

³Academy of Science, Physics Institute,
Baku 370143, Azerbaijan Republic

⁴Middle East Technical University,
Physics Department, 06531 Ankara, Turkey

Abstract

Dependences of the X-ray luminosity (L_x) of single pulsars, due to ejection of relativistic particles, on electric field intensity, rate of rotational energy loss (\dot{E}), magnetic field, period, and the energy spectra

*e-mail:huseyin@gursey.gov.tr

†e-mail:askin@gursey.gov.tr

‡email:physic@lan.ab.az

§email:ozgur@astroa.physics.metu.edu.tr

of the ejected particles are discussed. Influence of the magnetic field and effects of some other parameters of neutron stars on the L_x - \dot{E} and the L_x - τ (characteristic time) dependences are considered. Evolutionary factors also play an important role in our considerations. We find that only the pulsars with $L_{2-10\text{keV}} > 10^{33}$ erg/s have pulsar wind nebula around them. The pulsars from which γ -ray radiation has been observed have low X-ray luminosities in general.

Key words: Pulsar, SNR, X-ray

1 Introduction

It is well known that X-ray luminosities (L_x) of single neutron stars strongly depend on the rate of rotational energy loss (\dot{E}) ^{1,2,3}. \dot{E} depends on the spin period (P) and time derivative of the spin period (\dot{P}) of neutron stars. As there exist many other parameters of pulsars determined from P and \dot{P} values, L_x must also depend on these parameters. Naturally, these dependences can have different degrees and so must L_x depend on some of them strongly and on some of them weakly. This problem has already been analysed using values of L_x in 2-10 keV band for different groups of pulsars including also

the old millisecond pulsars ². We also prefer to use the L_x values in the 2-10 keV band, because the absorption is strong for softer X-ray band which may complicate the problem. Below, using reliable distance values we have analysed in detail the dependence of $L_{2-10keV}$ on different pulsar parameters for all single pulsars for which the radiation is related to ejection of relativistic particles. In this investigation we have also used the values of pulsar radiation in 0.1-2.4 keV band and the radiation of pulsar wind nebulae (PWNe) in both bands. Special attention has been paid to the evolutionary factors. There exist many pulsars with large values of \dot{E} and small values of age from which no X-ray radiation has been observed. Below, we have also discussed possible reasons of this.

2 Dependences of X-ray radiation of pulsars and their wind nebula on different parameters of pulsars

For the pulsed radio emission to occur and in order to produce radiation (excluding cooling radiation) in X-rays and also to form PWN, there must be

ejection of high-energy particles. The production of these kinds of radiation and PWN must depend on different parameters of neutron star. Note that the magnetic field may not be pure magneto-dipole field and the angle between the magnetic field and the spin axis is uncertain. These facts also make the solution of the problems more difficult. We want to figure out whether X-ray radiation of pulsars and the formation of PWN depend on \dot{E} or the electric field intensity (E_{el}) more strongly for the case of pure magneto-dipole radiation. In order to clarify these problems, we have constructed X-ray luminosity (2-10 keV) versus \dot{E} diagram for all radio and single X-ray pulsars with characteristic time (τ) $< 10^6$ yr located up to 7 kpc from the Sun including also 2 pulsars in Magellanic Clouds (Figure 1). The data of these pulsars are represented in Table 1.

Depending on values of the magnetic field and the speed of rotation on the surface of neutron star, there arises induced electric field of which the intensity is represented as ⁴:

$$E_{el} = \frac{4\pi R}{c} \frac{B_r}{P} \quad (1)$$

where R is the radius of neutron star, B_r the value of the real magnetic field strength and c the speed of light. As the P- \dot{P} diagram which we use is always

represented in logarithmic scale, the lines of constant E_{el} pass parallel to the lines of constant characteristic time

$$\tau = \frac{P}{2\dot{P}} \quad (2)$$

so that, we do not show the lines of $E_{el}=\text{constant}$ on the $P-\dot{P}$ diagram.

Often, there is PWN around such young pulsars which we include in Table 1. For such cases the X-ray luminosity value include both the X-ray radiation of the pulsar and of the PWN in most of the cases (particularly for the youngest pulsars), as it is difficult to distinguish the $L_x(\text{PWN})$ part of the luminosity. On the other hand, since the contribution of the PWN to the X-ray luminosity can be at most comparable with the X-ray luminosity of the pulsar in general ³, the change in the positions of the pulsars in the figures will be small in such cases that the dependences found from the best fits do not change considerably. It must also be noted that the uncertainties in the distance values and in the measured 2-10 keV fluxes can not have significant influences on these dependences. The pulsars with $\tau < 10^6$ yr located up to 7 kpc for which the X-ray luminosity in the 0.1-2.4 keV band is known are also shown in Table 1. We have adopted reliable values of distance for the pulsars ⁵ and X-ray luminosity data mainly have been taken from ² and ³.

We have preferred to use the data in 2-10 keV band (as in ²) instead of 0.1-2.4 keV band in order to get rid of the selection effects (e.g. absorption, cooling radiation, the radiation of the ejected relativistic particles being "harder", etc.).

The dependence between X-ray luminosity (2-10 keV) and \dot{E} is displayed in Figure 1 and the equation of this dependence is:

$$L_{2-10keV} = 10^{-23.40 \pm 4.44} \dot{E}^{1.56 \pm 0.12}. \quad (3)$$

In Figure 2, X-ray luminosity (2-10 keV) versus τ diagram is represented for the same pulsar sample shown in Figure 1. The equation for the relation between X-ray luminosity (2-10 keV) and τ is:

$$L_{2-10keV} = 10^{41.79 \pm 1.04} \tau^{-1.98 \pm 0.23}. \quad (4)$$

In order to see clearly whether the best fit of L_x vs. \dot{E} is better or worse than the best fit of L_x vs. τ (i.e. to make a comparison between Figure 1 and Figure 2 easily), we have used the same scales for the axes in Figures 1 and 2. As seen from Figures 1 and 2, the deviations of the data with respect to the best fits shown in the figures are larger in the L_x (2-10 keV) versus τ diagram compared to L_x (2-10 keV) versus \dot{E} diagram, but there is no significant difference. Since τ is proportional to $1/P$, whereas, \dot{E} is

proportional to $1/P^3$, two pulsars having approximately the same τ value with a large difference in their L_x (2-10 keV) values have positions in the L_x (2-10 keV)- \dot{E} diagram (Figure 1) with smaller deviations from the fit. This happens because the position of the pulsar with smaller value of P (large value of L_x) must shift to right and the one with larger value of P (small value of L_x) must shift to left approaching the best fit line in Figure 1.

Some pulsars in Table 1 have γ -ray radiation. As seen from Figure 1, these pulsars are in general located below the best fit line. On the other hand, all the pulsars with large effective magnetic field (B) values ($\log B > 12.7$) are located above the line (note that when there exist some additional mechanisms other than the magneto-dipole mechanism, $B > B_r$). We have not designated these pulsars in Figure 2 but notice that γ -ray pulsars in this figure are located in both parts with respect to the best fit line, whereas, all the pulsars with large values of B have positions below the line. This is also the result of different dependences of τ (see expression (2)), rate of rotational energy loss

$$\dot{E} = \frac{4\pi^2 I \dot{P}}{P^3}, \quad (5)$$

and

$$B = \sqrt{\frac{3c^3 I P \dot{P}}{8\pi^2 R^6}} \quad (6)$$

on values of P and \dot{P} (note that in this approximation we neglect the dependences of the observational and the calculated parameters of pulsars on the radius and mass of neutron stars). Here, the I is the moment of inertia of pulsar. \dot{E} always reflects the real rotational energy loss, but τ does not often reflect the real age for very young pulsars. For such pulsars there can be some additional torques other than the magneto-dipole radiation torque and their braking indices can be $n < 3$. Value of B which is estimated from eqn.(6) may be greater than the real value and the real age may be larger than the τ value. In actuality, not the τ but the real age values should be shown in Figure 2. Since the real age may be larger than τ , the pulsars with large values of B must shift to the part of larger τ and the deviations in Figure 2 must diminish. Please be aware that differences between the value of the real age and the τ value are different on different parts of the P - \dot{P} diagram. That is to say for different pulsars the difference between the real age and τ will be different depending on the braking index (i.e. the slope of the track).

Which parameters of neutron stars do the deviations in Figures 1 and 2

mainly depend on? In order to understand this, we have examined pulsars in narrow \dot{E} intervals with large differences in their L_x values which lead to large deviations. The largest deviation is for the interval $\log \dot{E}=36.78-36.9$ where pulsars J1846-0258, J1811-1925, and Vela are present. These are not ordinary pulsars: pulsars J1846-0258 and J1811-1925 are strong X-ray pulsars which have not been detected in other bands, whereas, Vela pulsar, which has been known as a radio, optical and gamma-ray pulsar until recently, has been identified also in X-rays but with low luminosity ⁶. The L_x (2-10 keV) value of Vela pulsar (Table 1) is more than one order of magnitude larger than the value given by ². This is because we have also included the X-ray luminosity of the PWN around the Vela pulsar which is about 10 times greater than the X-ray luminosity of the pulsar ⁷ and we have adopted a more reliable distance value ⁵ so that the luminosity value also increased about 3 times. Despite these facts, the position of Vela pulsar in Figure 1 is still well below the line and the difference between the luminosity values of Vela pulsar and pulsar J1846-0258 is still very large. Although, the period value of pulsar J1846-0258 is 4-5 times larger than the period values of Vela pulsar and pulsar 1811-1925, since B and \dot{E} values of pulsar J1846-0258 are larger than the values of the other two pulsars (even though the τ value is small), its

luminosity (2-10 keV) value is larger (see Table 1).

The second largest deviation among large \dot{E} values in Figure 1 is in the $\log \dot{E}=37.21-37.42$ interval where pulsars J1513-5908, J0205+6449, J1617-5055, and J2229+6114 are located in. Pulsar J1513-5908, the youngest one among these pulsars, has the largest P , B and L_x values. Among the other pulsars in this group, the largest \dot{E} value belongs to pulsar J0205+6449 in this interval and this pulsar has a smaller value of τ , a larger value of B , and a period value in between the values of pulsars J1617-5055 and J2229+6114. In spite of this, the luminosity of this pulsar is less than the luminosity of pulsar J1617-5055. This is strange, because all four parameters (P , τ , B , \dot{E}) of pulsar J0205+6449 suggest a larger luminosity value. Furthermore, there is no supernova shell or PWN around pulsar J1617-5055. This contradiction is not because of the adopted distance values. Is this contradiction related to the uncertainties in the observational data? Although, the luminosity values of these 2 pulsars (J0205+6449 and J1617-5055) are comparable within error limits ², one still can not explain why pulsar J0205+6449 does not have a larger L_x value. If the observational data are not significantly different than the actual values, then either there may be a considerable difference in the mass values of these 2 pulsars or the magnetic field may not be pure dipolar

field.

There are large deviations also in the small \dot{E} value part of Figure 1 where pulsars with $10^5 < \tau < 10^6$ yr values are located in. These pulsars do not eject enough number of relativistic particles, there is no PWN around them and the main radiation mechanism for them may be the cooling radiation. Because of this, the value of the X-ray luminosity should mainly depend on age, so that, we will examine these pulsars in the discussion of the deviations in Figure 2.

Among the youngest pulsars, the largest deviations are in the $\log \tau = 3.19 - 3.22$ interval. Among the pulsars in this interval, the smallest P and the largest \dot{E} values belong to pulsar J0540-6919 which has the largest L_x value. In this interval, the smallest L_x value belongs to pulsar J1119-6127 which has the largest P and B values and the smallest \dot{E} value. According to ⁸ J1119-6127 has unabsorbed L_x (0.5-10 keV) = $5.5_{-3.3}^{+10} \times 10^{32}$ erg/s at 6 kpc. There is no pulsed X-ray radiation observed from radio pulsar J1119-6127 and the position of the X-ray source is not coincident with the position of the radio pulsar; the observed point source may actually be a PWN ⁹.

Pulsar J1302-6350 and Geminga pulsar have $\log \tau = 5.52$ and $\log \tau = 5.53$, respectively. The period value of Geminga is about 5 times larger than the period of pulsar J1302-6350 and the \dot{E} value of Geminga is about 25 times

smaller than the \dot{E} value of J1302-6350. The X-ray luminosity of Geminga is more than 3 orders of magnitude less than the L_x value of J1302-6350. This is a very large difference. Please remember that pulsar J1302-6350 is in a binary system with a Be-star companion, so that, there may be some contribution to its X-ray luminosity.

Pulsar J0358+5413 has $\log \tau = 5.75$ and pulsar J0538+2817 has $\log \tau = 5.79$. The L_x value of pulsar J0358+5413 is about 300 times larger than the L_x value of pulsar J0538+2817, but the P, B and \dot{E} values of these 2 pulsars are roughly the same. Why is pulsar J0358+5413 much more luminous than pulsar J0538+2817? The absolute error of the L_x (2-10 keV) value of pulsar J0358+5413 is very large ² and the L_x (2-10 keV) value is not a directly measured value but converted by ² from the L_x value in softer band ¹⁰. So, the high L_x (2-10 keV) value of pulsar J0358+5413 can actually be much lower and the large difference in the L_x (2-10 keV) values of pulsars J0358+5413 and J0538+2817 can actually be much smaller.

Similarly, there are 2 other pulsars, namely J1124-5916 and J1826-1334, for which the uncertainties in their L_x (2-10 keV) values are very large. Pulsar J1124-5916 is located close to the best fit lines in Figures 1 and 2, whereas, pulsar J1826-1334 is located above and comparably farther away from the

lines in both figures. The positions of pulsar J1826-1334 in both figures do not create deviations and do not lead to contradictions as opposed to the cases discussed above. If the actual L_x (2-10 keV) value of this pulsar is half of the value given in Table 1, then the positions of it in the figures can be considered absolutely normal.

If we consider the corrections to the positions of some of the pulsars discussed above taking also into account relations between L_x and \dot{E} , τ , B and P , and if we change the positions of the pulsars in the figures within error limits given in ² then, pulsar J1119-6127 will have a higher L_x value, pulsars J1826-1334, J1302-6350 and J0358+5413 will have lower values of L_x . In this case, the dependence between L_x and τ given in eqn.(4) will be improved with a more negative power of τ . If we apply the same approach for the positions of some of the pulsars in Figure 1, we see that the deviations do not decrease and the power of \dot{E} (eqn.(3)) increases negligibly. On the other hand, from Eqns (3) and (4) we see that L_x is more sensitive to changes in τ compared to changes in \dot{E} .

As seen from Figures 1,2 and Eqns. (3) and (4), on the average, the pulsars with small τ (or large E_{el}) and large \dot{E} values have considerably large X-ray luminosity in the 2-10 keV band. From Figures 1 and 2, it is seen

that the magnitude of the deviations practically do not depend on \dot{E} or τ along the lines. Since the temperature of the neutron star is related to τ , we can say that the deviations can not be explained by the temperature, so that, the existence of such deviations must be due to some other parameters. Note that there are also some pulsars in Figure 2 with large values of τ for which the influence of the cooling radiation to their X-ray radiation is large. Therefore, L_x values of pulsars with ages 10^5 - 10^6 yr must considerably decrease, but this is not seen clearly.

We have not included the millisecond pulsars with $\tau > 10^6$ yr in Table 1 nor in the figures, because the origin of such pulsars is different. The pulsars in our sample were born as single (with one exception which is the case of a pulsar with a Be-type companion in a wide binary system. Note that this binary system has not evolved through X-ray binary stage) roughly in the upper left part of the P - \dot{P} diagram, whereas, the birth place of old millisecond pulsars on the P - \dot{P} diagram is highly uncertain.

Some of the pulsars shown in Figures 1,2 and in Table 1 have experienced strong glitches ($\frac{\Delta P}{P} > 10^{-6}$, denoted with 'G' in Figure 2). As seen from Figure 2, the deviations of the data do not seem to be due to the glitches, either (this is also true for Figure 1 where we have not denoted such pulsars).

3 The evolutionary factors

Since the values of P and \dot{P} and all the other parameters change continuously during the pulsar evolution, the value of $L_{2-10keV}$ must also change in connection to this. We want to analyse how the $L_{2-10keV}$ luminosity of pulsars changes during the evolution of pulsars on the P - \dot{P} diagram.

From eqn. (3) we see that

$$L_{2-10keV}^{(\dot{E})} \propto \left(\frac{\dot{P}}{P^3}\right)^{1.56} \quad (7)$$

and similarly from eqn. (4)

$$L_{2-10keV}^{(\tau)} \propto \left(\frac{\dot{P}}{P}\right)^{1.98} \quad (8)$$

using the expressions for \dot{E} (5) and τ (2). Now, using the expression for B (6), we can write (7) and (8) in the form:

$$L_{2-10keV}^{(\dot{E})} \propto \left(\frac{B^2}{P^4}\right)^{1.56} \quad (9)$$

and

$$L_{2-10keV}^{(\tau)} \propto \left(\frac{B^2}{P^2}\right)^{1.98}. \quad (10)$$

If both dependences (3) and (4) are applicable in finding the value of L_x , then the ratio of the luminosities for each pulsar found from equations (9)

and (10) must roughly be the same throughout the evolution of a pulsar.

From dependences (10) and (9) we get:

$$\frac{L_{2-10keV}^{(\tau)}}{L_{2-10keV}^{(\dot{E})}} \propto B^{0.84} P^{2.28}. \quad (11)$$

So, the ratio is strongly dependent on P which must be wrong because the ratio must not change significantly during the evolution if both dependences are reliable.

X-ray luminosity of the considered pulsars strongly depends on different parameters of pulsars and decreases with age down to $L_x \sim 10^{29}-10^{30}$ erg/s. During the evolution of these pulsars, the period value changes up to a factor of 10, \dot{P} up to 50 times, \dot{E} up to 10^4 times, and τ up to 10 times. (The initial values of τ for the pulsars we analyse are in the interval 10^3-10^5 yr independent of the value of B . There are no X-ray data for the earlier times of the pulsar groups each of which include pulsars with B values close to each other). During the evolution, value of B for each pulsar may decrease only up to a factor of 3, but magnitudes of the deviation of P and \dot{P} and especially B values for different pulsars are larger.

As seen from Figure 5, an increase in the initial magnetic field value of a factor of 10 leads to a decrease in the lifetime of X-ray pulsar of a factor of 10

and this is related to a rapid increase in the value of P . As X-ray luminosity of pulsars strongly depends on E_{el} and \dot{E} , as seen from the $L_x-\tau$ diagram (Figure 2) and Figure 5, the X-ray luminosities of the pulsars with largest initial B values drop very quickly below the threshold during the evolution, whereas, the X-ray luminosities of the pulsars with smaller initial values of B last longer and drop below the threshold in about 10^5 yr. Pulsars with larger values of B , in contrast to pulsars with smaller B values, have PWNe and large values of L_x . Therefore, they may be observable even if they are located at large distances. In spite of this, their number is small because they evolve fastly on the $P-\dot{P}$ diagram. Pulsars with small values of B have low birth rates and small values of L_x . They are located on different parts of $L_x-\tau$ diagram but they are located along all parts of the best fit line on the $L_x-\dot{E}$ diagram. Therefore, it is necessary to consider a more homogeneous group of pulsars which have B values close to each other. Naturally, the best fit lines for the new sample must lead to a different equation for the $L_x-\tau$ dependence and practically the same equation for the $L_x-\dot{E}$ dependence.

We have found the dependences (3) and (4) using the whole pulsar sample in Figures 1 and 2. In other words, we have used the data of the pulsars which have B values in a wide range. In order to clarify the evolutionary effects

it is necessary to consider pulsars with B values in a narrower interval (i.e. the pulsars with evolutionary tracks close to each other). By this way, we decrease the influences of the very wide-range initial values of B and P on dependences (3) and (4). Dependence (4) must change more because of the considerable decrease in the range of P also. In order to see this, we have constructed L_x vs. \dot{E} and L_x vs. τ diagrams (Figures 3 and 4) for the pulsars with B values in the interval $12.2 \leq \log B \leq 12.7$ (Figure 5). About half of the pulsars shown in Figures 1 and 2 have B values in this interval. Again from the best fits, we get dependences between L_x and \dot{E} :

$$L_{2-10keV} = 10^{-27.46 \pm 6.48} \dot{E}^{1.66 \pm 0.18} \quad (12)$$

and L_x and τ :

$$L_{2-10keV} = 10^{45.98 \pm 1.51} \tau^{-2.99 \pm 0.36}. \quad (13)$$

From these two dependences it is seen that the dependence given by eqn.(3) is comparable to the dependence given by eqn.(12) within error limits, but the dependence given by eqn.(4) changed considerably (see eqn.(13)).

Dividing eqn.(13) by eqn.(12) and again using the expressions (5) and (2) we get:

$$\frac{L_{2-10keV}^{(\tau)}}{L_{2-10keV}^{(\dot{E})}} \propto B^{2.66} P^{0.66}. \quad (14)$$

If the effective B value decreases gradually during the evolution, the large increase in the P value compensates it and the ratio remains approximately the same. It must also be mentioned that we have done this analysis by adopting a narrower interval of B , because B values do not change much as the other parameters do during the evolution. The B values of the considered group of pulsars (we do not consider anomalous X-ray pulsars, soft gamma repeaters, and binary X-ray pulsars) can only decrease or remain constant throughout the evolution. In Figures 3 and 4, number of the X-ray pulsars is small and there are particularly small numbers of pulsars on the right and the left parts of both figures. Therefore, the dependences (12) and (13) have large uncertainties compared to the dependences (3) and (4). Nevertheless, they are more reliable as demonstrated by the dependences of L_x on \dot{E} and especially on τ (age), because we have used a more homogeneous group of pulsars with similar evolutionary tracks in Figures 3 and 4. The ratio given by dependence (14) shows this fact.

The reason of the considerable difference between the dependences (4) and (13) can easily be seen in Figure 5. As seen from this figure, when the value of τ is small, first the constant τ line crosses the considered B interval (i.e. the interval of $12.2 \leq \log B \leq 12.7$) where the value of \dot{E} is

large. Then, it crosses the region, which is not included in the B interval under consideration, where the value of \dot{E} is small. On the other hand, if the value of τ is large, then the constant τ line first crosses a region, outside the considered B interval, where pulsars with large values of \dot{E} are located, and then it crosses the B interval under consideration where pulsars with small \dot{E} values are present. Therefore, for small values of τ , the pulsars which have smaller values of $L_{2-10keV}$ and which are not located in the considered interval have positions below the best fit line in Figure 4. On the other hand, for large values of τ , the pulsars which have larger values of $L_{2-10keV}$ and which are not located in the considered interval have positions above the best fit line in Figure 4. These facts lead to the considerable difference between the dependences (4) and (13).

In Table 1, we have also included the 15 pulsars with $\tau < 10^5$ yr and/or $\log \dot{E} > 35.60$ from which no X-ray radiation has been detected. Within and around this region of the $P-\dot{P}$ diagram (see Figure 5), there are pulsars with detected X-ray radiation. All of these pulsars without detected X-ray radiation are also located at $d \leq 7$ kpc from the Sun. One of these pulsars is connected to a supernova remnant (SNR). In Figure 5, the $P-\dot{P}$ diagram for all the 48 pulsars in Table 1 is displayed. Please notice that, since the pulsar

sample used in Figure 5 includes also the pulsars without detected X-ray radiation and the pulsars with detected X-ray radiation only in the 0.1-2.4 keV band, it is not the same sample used in Figures 1 and 2.

As mentioned above, as τ increases and \dot{E} decreases, L_x considerably decreases (see Figures 1-4). It is also seen from Figure 5 that the ratio of the number of pulsars without detected X-ray radiation to the number of pulsars which have been detected in X-rays increases as τ increases and \dot{E} decreases. (Note that there exist more pulsars with ages 10^5 - 10^6 yr located at distances up to 7 kpc, but they are not included in Table 1, because they have not been observed in X-ray band and they are not connected to SNRs).

As seen from Figure 5 and Table 1, there are some pulsars without observed X-ray radiation which have smaller τ values and larger \dot{E} values compared to some pulsars with observed X-ray radiation. What is the reason for not detecting X-ray radiation from such pulsars? As mentioned in the previous section, the X-ray luminosity must depend not only on P and \dot{P} but also on some other parameters. The deviations of the data from the best fits in Figures 1-4 also show this fact. It is not easy to examine these "other parameters" which can not be calculated from values of P and \dot{P} and get reliable results. But it is possible to clarify why there exist those pulsars

with smaller τ values and larger \dot{E} values from which no X-ray radiation has been detected by examining the selection effects.

It is clear that it is more difficult to observe the X-ray radiation of a pulsar if it is located at a large distance in the Galactic plane and in the Galactic centre direction. All the 8 pulsars with $\tau > 10^5$ yr from which X-ray radiation has been observed as shown in Figure 5 are located < 2.5 kpc from the Sun (Figure 6). Directions of these and all the other pulsars in Table 1 are shown in b vs. l diagram (Figure 7).

In Figure 6, the dependence of \dot{E} on distance for all the 48 pulsars in Table 1 is represented. The pulsars without observed X-ray radiation are all located beyond 2 kpc from the Sun. It is normal to detect X-ray radiation from pulsars with large \dot{E} values even at large distances (see Figure 6), but there is a pulsar, namely J0631+1036, with detected X-ray radiation in the 2-10 keV band which is located at $d = 6.6$ kpc and has a smaller \dot{E} value ($\log \dot{E} = 35.24$). The reason for this is that this pulsar is located in the Galactic anti-centre direction (see Figure 7). The other 8 pulsars with detected X-ray radiation and with distances between 6-7 kpc are located in the Galactic central directions. Six out of the 8 far away pulsars in the central directions are connected to SNRs that these are well examined pulsars. So, it must be

considered normal to detect X-ray radiation from these pulsars even if they are located at large distances and in the Galactic centre directions. On the other hand, the remaining 2 pulsars, namely J1105-6107 and J1617-5055, are in the Galactic central directions and are not connected to SNRs. Pulsar J1617-5055 has very high \dot{E} and large L_x values (see Table 1), and pulsar J1105-6107 is located in between the Sagittarius and the Scutum arms so that it is normal to observe the X-ray emission of these 2 pulsars. All the pulsars without detected X-ray radiation are located in the central directions and in the directions of Vela OB-associations (see Figure 7). Moreover, the pulsars with $d \leq 4.1$ kpc which have not been detected in X-rays (J0940-5428, J1809-1917, J1718-3825, J1531-5610, J1509-5850, J1913+1011) have all been found in recent pulsar surveys ^{11,12,13}. In the near future, it is possible that all of these pulsars will be detected in X-rays.

As mentioned above, all the pulsars without detected X-ray radiation which have $\log \dot{E} > 35.60$ and/or $\log \tau < 5$ located up to 7 kpc are represented in Table 1. We have also examined the pulsars without detected X-ray radiation which have $\log \dot{E} < 35.60$ and $\log \tau < 5$ located up to 7 kpc in order to understand why X-ray radiation has not been detected from these pulsars. There are 18 such pulsars (which are not included in Table

1) and all of these pulsars have large B values ($\log B \geq 12.5$). This examination is important in order to bring to light which parameter the X-ray "death-belt" depends on for pulsars with large B values. Again, we see that it mainly depends on \dot{E} . Twelve out of these 18 pulsars are located beyond 4 kpc (pulsars J1841-0348, J1705-3950, J0729-1448, J0725-1637, J1841-0524, J1837-0604, J1718-37184, J1702-4128, J1626-4537, J0901-4624, J1638-4608, J1737-3137) and all of these 12 pulsars have been found in recent surveys^{5,14}. Only from 2 of the 12 pulsars (J0729-1448 with $l=230^\circ.39$, $b=1^\circ.42$ and J0725-1637 with $l=231^\circ.5$, $b=-0^\circ.3$) one can expect to observe X-ray radiation (if it exists) relatively easily; these 2 pulsars are located in Galactic anti-centre directions, whereas, the other 9 pulsars are all in the Galactic central directions with small b values. On the other hand, if we compare pulsars J0729-1448 and J0725-1637 with the pulsars with detected X-ray radiation which have similar \dot{E} values ($\dot{E} < 35.5$, see Figure 1 and Table 1) we see that it is not so easy to detect X-ray radiation from such pulsars if they are located beyond 3 kpc. But there is one exception which we have discussed above, namely pulsar J0631+1036 (see Figures 6 and 7). So, it is important to observe pulsars J0729-1448 and J0725-1637 to detect X-ray radiation.

Seven of the 18 pulsars are located less than 4 kpc from the Sun and all

of them have $\log \dot{E} \leq 35.0$ (pulsars J1918+1414, J1740-3015, J1913+0446, J1601-5335, J1731-4744, J0614+2229, J1738-2955). Also, their spin periods are larger (note that as period increases the X-ray radiation decreases). If we consider the fact that six of these 7 pulsars are located beyond 3 kpc together with the small values of \dot{E} and large values of P we can say that it is difficult to observe X-ray radiation from these pulsars. The remaining pulsar (J1918+1444) is located at $d = 1.2$ kpc, but as it has $\log \dot{E} = 33.7$ and $P = 1.18$ s we do not expect this pulsar to be detected in X-rays, either; it can not eject enough number of relativistic particles and produce X-ray radiation.

4 Conclusions

Investigations of single pulsars which radiate X-rays as a result of ejection of relativistic particles show that:

- 1) Luminosity in 2-10 keV band (often the total luminosity including the luminosity of the PWN) strongly depends on electric field intensity E_{el} (or age), rate of rotational energy loss \dot{E} , magnetic field B , period, and energy spectra of the ejected particles.

2) The dependence of L_x on \dot{E} is practically the same for pulsars with very different values of B and with $B=10^{12}-10^{13}$ G. This is not true for the $L_x-\tau$ dependence.

3) Pulsars with different initial values of B at ages about 10^3 yr begin to evolve from different points of the $L_x-\dot{E}$ dependence and then continue to evolve with similar trajectories until L_x drops to $\sim 10^{30}$ erg/s, but the same pulsars begin and end their evolution in different parts of the $L_x-\tau$ dependence and the evolutionary tracks are not parallel to the $L_x-\tau$ dependence for all the pulsars under consideration.

4) The pulsars which also radiate gamma-rays, with the same values of \dot{E} as the other pulsars without gamma-ray radiation, have several times smaller X-ray luminosities.

5) The pulsars which have PWNe practically always have X-ray luminosities greater than 10^{33} erg/s.

6) Practically, values of τ and \dot{E} determine the X-ray luminosity. The increase in τ and the decrease in \dot{E} simultaneously lead to a rapid decrease in L_x . Value of L_x decreases from $\sim 10^{37}$ erg/s for $\dot{E} \sim 3 \times 10^{38}$ erg/s and $\tau \sim 10^3$ yr to $\sim 10^{30}$ erg/s for $\dot{E} \sim 3 \times 10^{34}$ erg/s and $\tau \sim 3 \times 10^5$ yr.

It is necessary to reexamine the X-ray flux values of J0205+6449, J0358+5413,

and J0538+2817 in 2-10 keV band to understand the dependence of the X-ray luminosity on \dot{E} , E_{el} , B and P values and the possible dependence on the energy spectra of the ejected particles.

Also, in order to understand the dependence of the X-ray radiation on different parameters of pulsars better, it is necessary to observe pulsars J0940-5428, J1809-1917, J1718-3825, J1531-5610, J1509-5850, J1913+1011, and particularly J0729-1448 and J0725-1637 with X-ray telescopes, preferably in the hard X-ray band.

Acknowledgments We would like to thank Efe Yazgan for his valuable comments.

References

1. Becker, W. and Trumper, J., A&A **326**, 682 (1997).
2. Possenti, A., Cerutti, R., Colpi, M. and Mereghetti, S., A&A **387**, 993 (2002).
3. Becker, W. and Aschenbach, B., Proceedings of the 270. WE-Heraeus Seminar on: "Neutron Stars, Pulsars and Supernova Remnants", eds. W. Becker, H. Lesch and J. Trumper, MPE Report **278**, p.64 (2002).
4. Lipunov, V. M., Astrophysics of neutron stars, Springer-Verlag (1992).
5. Guseinov, O. H., Yerli, S. K., Ozkan, S., Sezer, A. and Tagieva, S. O., accepted for publication by Astron. and Astrop. Transac. (2003), (astro-ph/0206050).
6. Lyne, A. G. and Graham-Smith, F., Pulsar astronomy, Cambridge University Press (1998).
7. Pavlov, G. G., Kargaltsev, O. Y., Sanwal, D. and Garmire, G. P., ApJ **554**, L189 (2001).
8. Gonzalez, M. and Safi-Harb, S., ApJ **591**, L143 (2003).
9. Pivovaroff, M. J., Kaspi, V. M., Camilo, F., Gaensler, B. M. and Crawford, F., ApJ **554**, 161 (2001).

10. Sun, X., Anderson, S., Aschenbach, B., et al., Proc. 'Rontgenstrahlung from the Universe', eds. Zimmermann, H. U., Trumper, J. and Yorke, H., MPE Report **263**, p.195 (1996).
11. Manchester, R. N., Lyne, A. G., Camilo, F., et al., MNRAS **328**, 17 (2001).
12. Morris, D. J., Hobbs, G., Lyne, A. G., et al., MNRAS **335**, 275 (2002).
13. Kramer, M., Bell, J. F., Manchester, R. N., et al., MNRAS **342**, 1299 (2003).
14. ATNF Pulsar Catalogue (2003), (<http://www.atnf.csiro.au/research/pulsar/psrcat/>).
15. Helfand, D. J., Collins, B. F. and Gotthelf, E. V., ApJ **582**, 783 (2003).
16. Lorimer, D. R., Lyne, A. G. and Camilo, F., A&A **331**, 1002 (1998).
17. Allakhverdiev, A. O., Alpar, M. A., Gok, F. and Guseinov, O. H., Turkish Jour. of Phys. **21**, 688 (1997).
18. Seward, F. D., Harnden, F. R. Jr. and Helfand, D. J., ApJ **287**, L19 (1984).
19. Kothes, R., Uyaniker, B. and Pineault, S., ApJ **560**, 236 (2001).
20. Manchester, R. N., Bell, J. F., Camilo, F., et al., Neutron Stars in Supernova Remnants, ASP Conference Series, edited by Patrick O. Slane

and Bryan M. Gaensler, **271**, p.31 (2002).

21. Thorsett, S. E., Brisken, W. F. and Goss, W. M., *ApJ* **573**, L111 (2002).
22. Frail, D. A., Goss, W. M. and Whiteoak, J. B. Z., *ApJ* **437**, 781 (1994).
23. Camilo, F., Bell, J. F., Manchester, R. N., et al., *ApJ* **557**, L51 (2001).
24. Kaspi, V. M., Roberts, M. E., Vasisht, G., Gotthelf, E. V., Pivovaroff, M. and Kawai, N., *ApJ* **560**, 371 (2001).
25. Furst, E., Reich, W. and Seiradakis, J. H., *A&A* **276**, 470 (1993).

Figure Captions

Figure 1: Log L_x (2-10 keV) versus $\log \dot{E}$ diagram of all 30 pulsars with $\tau < 10^6$ yr which have observed X-ray radiation. 28 of these pulsars are located up to 7 kpc from the Sun and 2 of them are in Magellanic Clouds. 'Plus' signs denote the 2 pulsars in Magellanic Clouds. 'Cross' signs show the positions of pulsars with $10^5 < \tau < 10^6$ yr and 'star' signs show the positions of pulsars with $\tau < 10^5$ yr. 'Square' signs denote single X-ray pulsars. Seven of these pulsars have $\log B > 12.7$ (denoted with 'B') and from 8 of them γ -rays have been observed (denoted with 'G').

Figure 2: Log L_x (2-10 keV) versus $\log \tau$ diagram of all 30 pulsars with $\tau < 10^6$ yr which have observed X-ray radiation. 28 of these pulsars are located up to 7 kpc from the Sun and 2 of them are in Magellanic clouds. 'Plus' signs denote the 2 pulsars in Magellanic Clouds. 'Cross' signs show the positions of pulsars with $10^5 < \tau < 10^6$ yr and 'star' signs show the positions of pulsars with $\tau < 10^5$ yr. 'Square' signs denote single X-ray pulsars. Seven of these pulsars have experienced strong ($\Delta P/P > 10^{-6}$) glitches (denoted with 'G').

Figure 3: Log L_x (2-10 keV) versus $\log \dot{E}$ diagram for 15 of the 30 pulsars shown in Figures 1 and 2; these 15 pulsars have $12.2 \leq \log B \leq 12.7$. 'Plus' sign denotes the pulsar in Magellanic Cloud. 'Cross' signs show the positions

of pulsars with $10^5 < \tau < 10^6$ yr and 'star' signs show the positions of pulsars with $\tau < 10^5$ yr. 'Square' sign denotes the single X-ray pulsar.

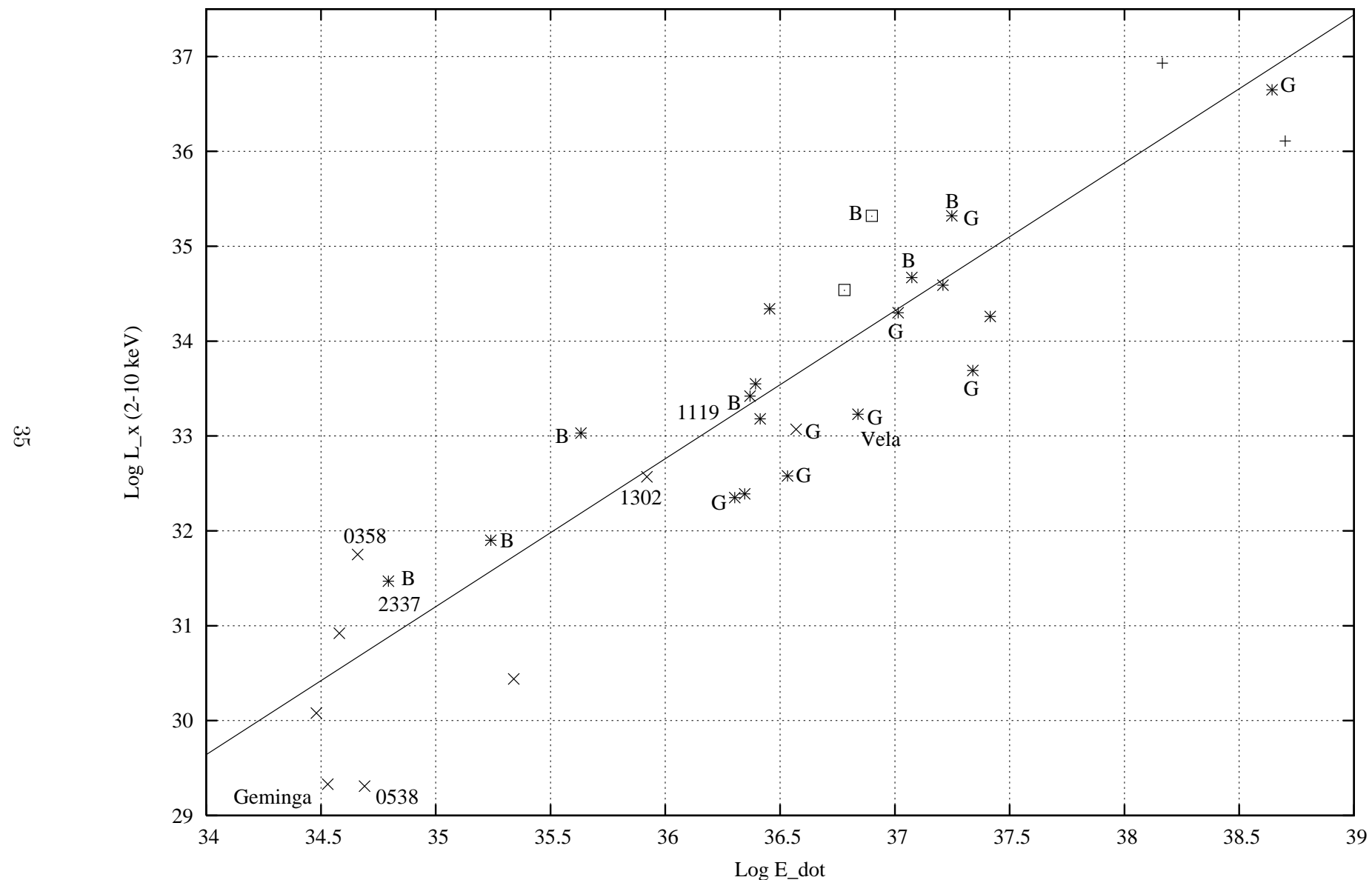
Figure 4: Log L_x (2-10 keV) versus $\log \tau$ diagram for 15 of the 30 pulsars shown in Figures 1 and 2; these 15 pulsars have $12.2 \leq \log B \leq 12.7$. 'Plus' sign denotes the pulsar in Magellanic Cloud. 'Cross' signs show the positions of pulsars with $10^5 < \tau < 10^6$ yr and 'star' signs show the positions of pulsars with $\tau < 10^5$ yr. 'Square' sign denotes the single X-ray pulsar. Black squares show the positions of the pulsars which are present in Figure 2 but not included in the fit of Figure 4.

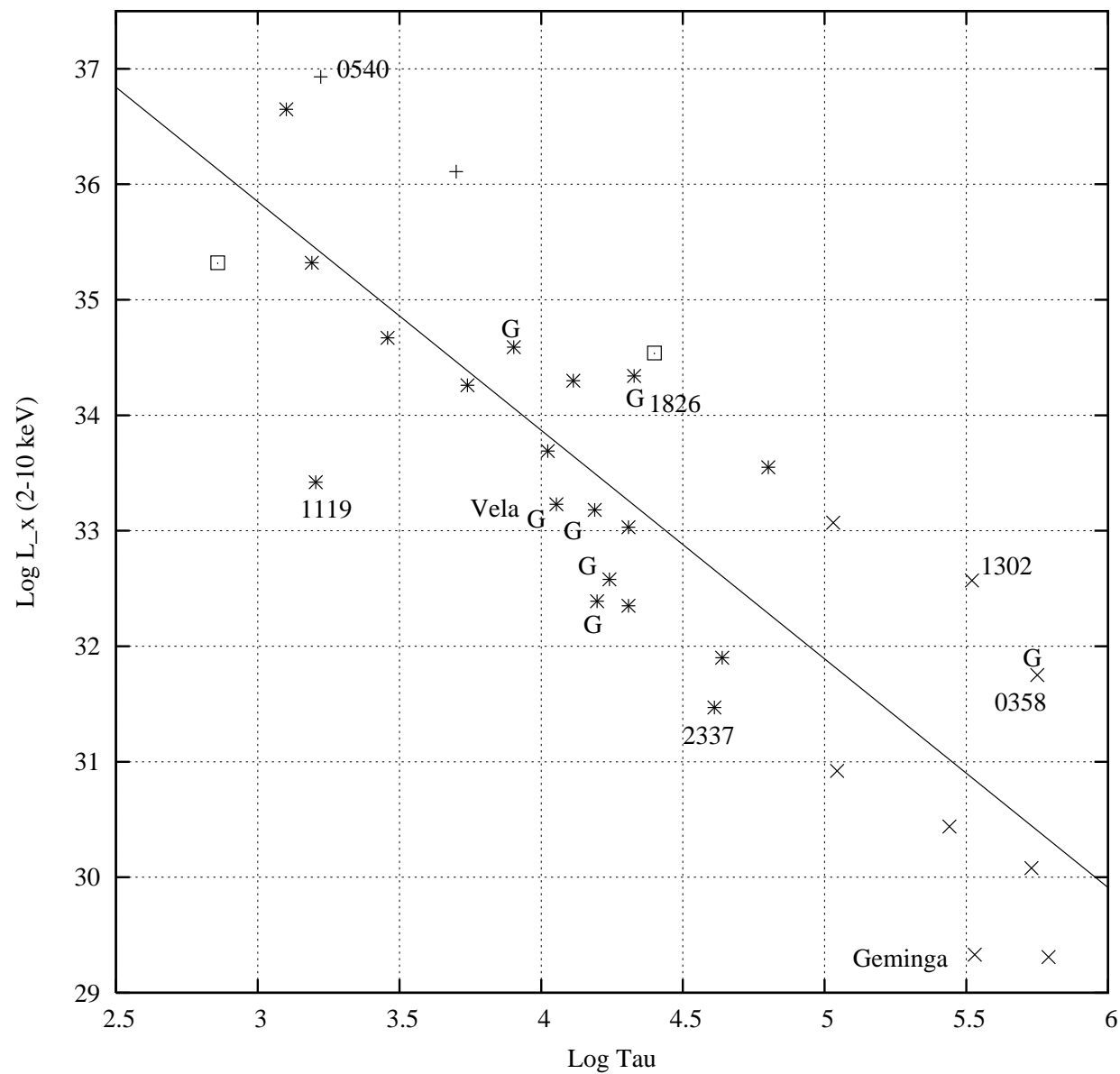
Figure 5: Period versus period derivative diagram for all 48 pulsars represented in Table 1 with $\tau < 10^6$ yr and distance ≤ 7 kpc including the 2 pulsars in Magellanic Clouds. 'Circles' represent the 33 pulsars from which X-ray radiation have been detected in 2-10 keV and/or 0.1-2.4 keV bands. 'Plus' signs denote the 15 pulsars with $\log \dot{E} > 35.55$ from which no X-ray radiation has been observed.

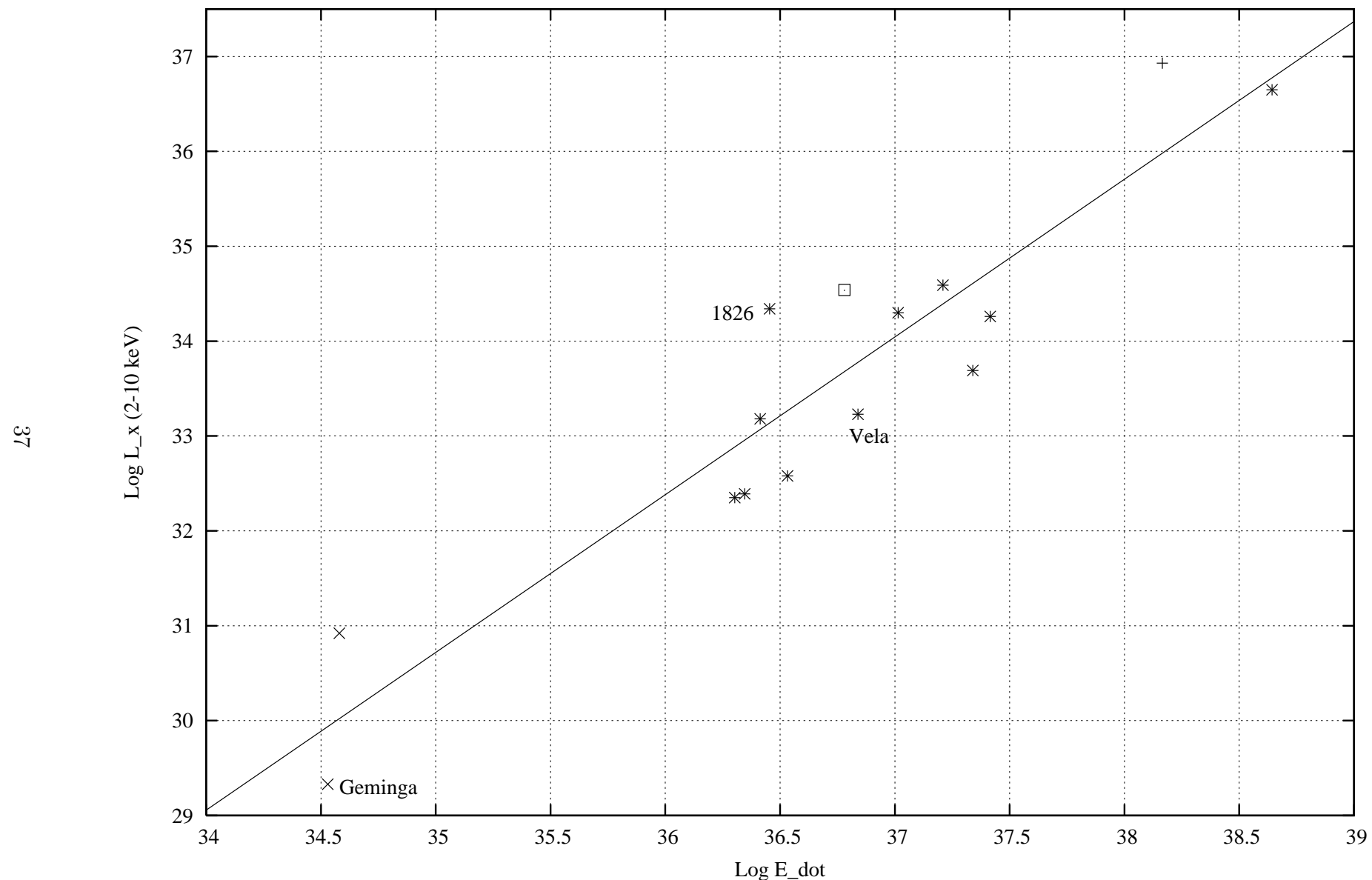
Figure 6: Log \dot{E} versus distance diagram for all 48 pulsars represented in Table 1 with $\tau < 10^6$ yr and distance ≤ 7 kpc including the 2 pulsars in Magellanic Clouds. 'Circles' represent the 33 pulsars from which X-ray radiation have been detected in 2-10 keV and/or 0.1-2.4 keV bands. 'Plus' signs

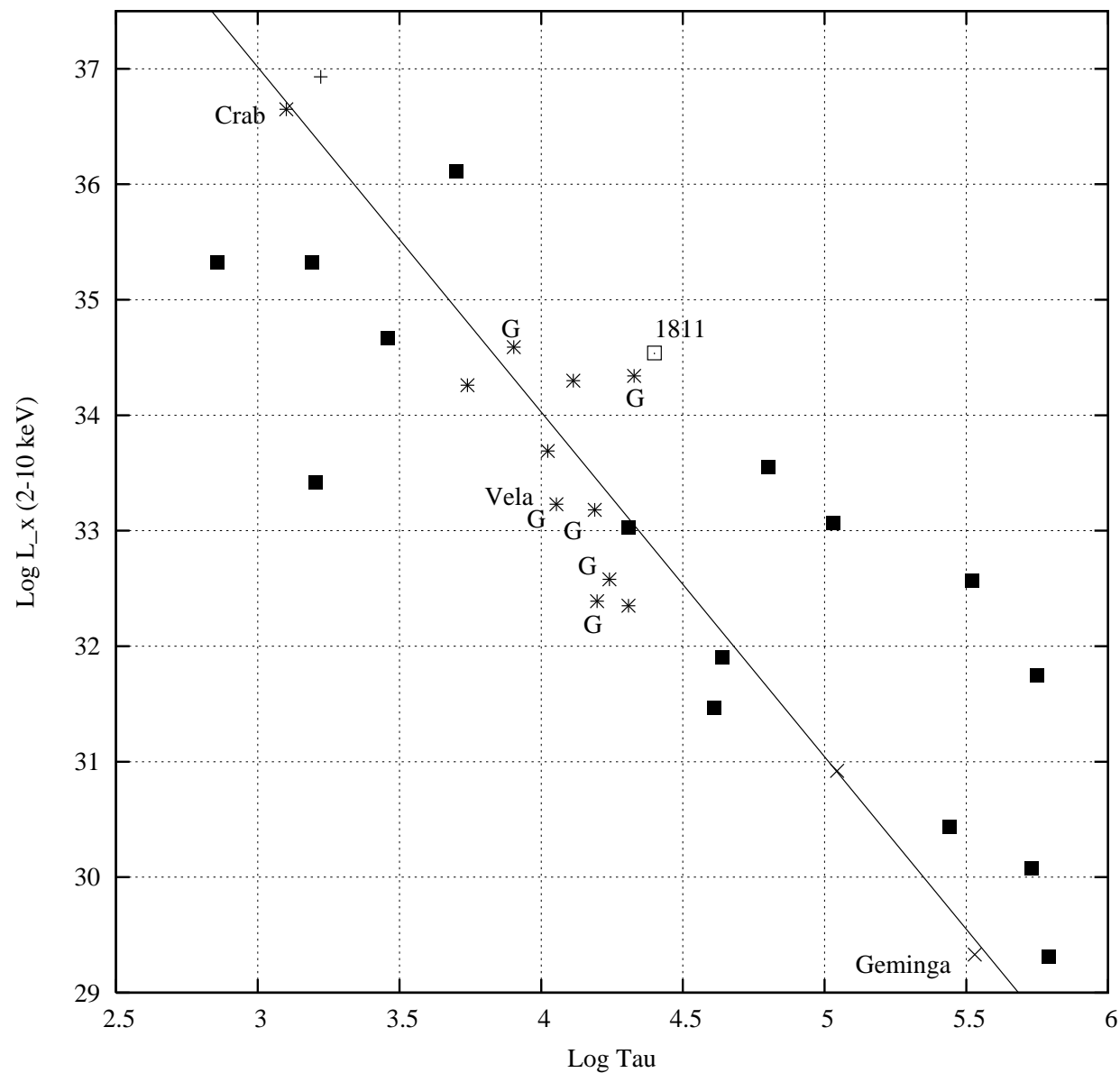
denote the 15 pulsars with $\log \dot{E} > 35.55$ from which no X-ray radiation has been observed. 'Cross' signs represent the 8 pulsars with $10^5 < \tau < 10^6$ yr.

Figure 7: Galactic longitude (l) versus Galactic latitude (b) diagram for all 48 pulsars represented in Table 1 with $\tau < 10^6$ yr and distance ≤ 7 kpc including the 2 pulsars in Magellanic Clouds. 'Circles' represent the 33 pulsars from which X-ray radiation have been detected in 2-10 keV and/or 0.1-2.4 keV bands. 'Plus' signs denote the 15 pulsars with $\log \dot{E} > 35.55$ from which no X-ray radiation has been observed. 'Cross' signs represent the 8 pulsars with $10^5 < \tau < 10^6$ yr.

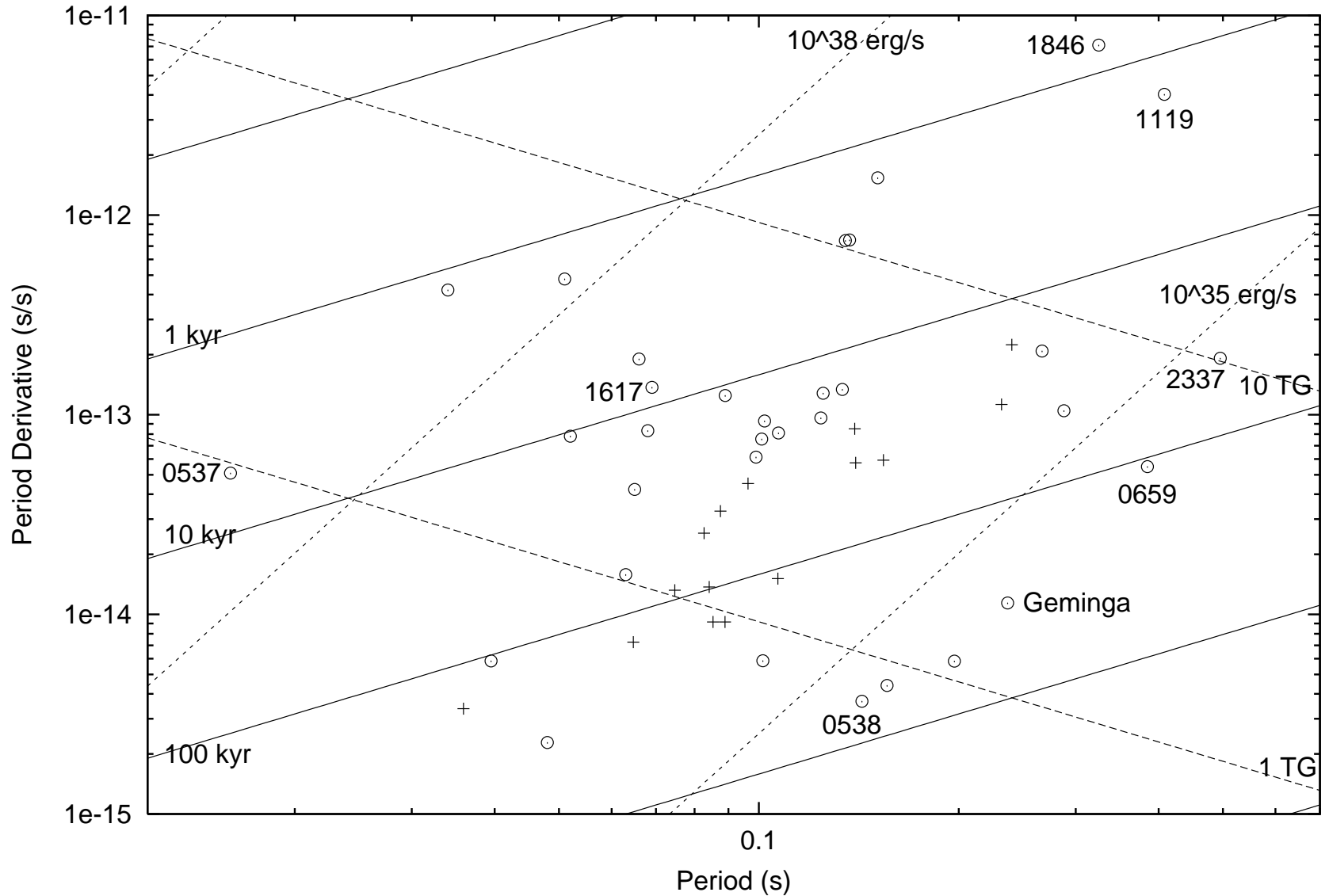








68



PSRs With X-ray Radiation(+) And PSRs With LogEdot>35,d<7,Tau<E6,No X-ray Radiation(circle)

